

34. PETROLOGY OF ULTRAMAFIC ROCKS FROM SITE 395

S. Arai,¹ Geological Institute, University of Tokyo, Tokyo, Japan
and

T. Fujii², Carnegie Institute, Geophysical Laboratory, Washington, D.C.

ABSTRACT

Serpentinized peridotites recovered at DSDP Site 395 preserve the original minerals: olivine, orthopyroxene, clinopyroxene, and chromian spinel. The estimated equilibration temperature indicates that they were equilibrated under upper-mantle conditions, and the compositions of constituent minerals indicate that they are residues left after removal of more fusible components as basaltic magmas. It is suggested, therefore, that they are the fragments of residual oceanic upper mantle, which were emplaced into oceanic crust as solid intrusion along faults.

They are mineralogically similar to the ultramafic tectonites of ophiolite complexes; this supports the hypothesis that ophiolite complexes are generated at or near the mid-oceanic ridges and that their ultramafic tectonites represent the oceanic upper mantle.

INTRODUCTION

On the basis of the similarity between the oceanic crust-mantle section, derived mainly from geophysical data, and the stratigraphic sequences of ophiolite complexes in orogenic regions, it is widely believed that ophiolite complexes are slices of the ancient oceanic plates (e.g., Coleman, 1971). Geochemical studies of basic rocks of ophiolite complexes support this hypothesis, and suggest that ophiolite complexes were formed at mid-oceanic ridges (e.g., Moores and Vines, 1971), although some ophiolite complexes might have been generated in other tectonic environments (Miyashiro, 1973).

The ultramafic rocks from oceanic regions may possibly be equivalent to the ultramafic rocks of ophiolite complexes (e.g., Prinz et al., 1976), but, detailed petrographical and mineralogical comparisons are still scarce. It is important, therefore, to compare the petrology of ultramafic rocks from the mid-oceanic ridges with that of ultramafic rocks in ophiolite complexes of orogenic regions. It is also important to understand the petrochemical and mineralogical characteristics of oceanic peridotites for further understanding of the oceanic crust and mantle.

Peridotites from Hole 395, Core 18, may be suitable for the above purposes, since they are relatively fresh, with original minerals preserved.

PETROGRAPHIC DESCRIPTION

Two samples were available from Core 395-18: 18-1, Piece 2C and 18-2, Piece 17B. Although according to the Leg 45 *Initial Core Descriptions* Samples 18-1, 2C is from a harzburgite zone and Sample 18-2, 17B is from a lherzolite zone, both seem to be lherzolite within the small available samples, and contain olivine, orthopyroxene, clinopyroxene, and spinel.

Sample 18-1, 2C is relatively fresh; 40 to 50 per cent serpentinized. Yellow to brown serpentine (lizardite-crysotile) has selectively replaced olivine, whereas pyroxenes are almost intact. Carbonate, magnetite, pyrrhotite, and clay minerals are present as alteration products. Brucite and amphibole are absent. Olivine contains lamellae of thin, parallel flakes of yellow-brown spinel. No definite relationship between the orientation of spinel flakes and the crystallographic direction of host olivine is evident, however. Olivine also includes irregularly shaped chromian spinels. Symplectite, possibly composed of chromian spinel and clinopyroxene, is occasionally present as thin plates in olivine. Orthopyroxene contains numerous fine lamellae of clinopyroxene in its central part. Clinopyroxene is round or irregular in shape, and in some cases interstitial to orthopyroxene and olivine. Conspicuous parting is commonly developed. Fine-grained irregular clinopyroxene intergrown with fine-grained chromian spinel is occasionally present. Large grains of brown chromian spinel also occur.

Sample 18-2, 17B is moderately to intensely serpentinized, and markedly deformed. Olivine rarely contains rods of chromian spinel. Pyroxenes are strongly bent and kinked, and show remarkable wavy extinction. Conspicuous parting is also evident. Exsolution la-

¹ Now at Geoscience Institute, Shizuoka University, Shizuoka, Japan.

² Now at Geological Institute, University of Tokyo, Tokyo, Japan.

mellae seem to be thicker than those in Sample 18-1, 2C, and often grow to exsolution blebs. Thin clinopyroxene occupies the crack produced by deformation of the orthopyroxene grain. The bent pyroxene grains are surrounded by fine-grained granular aggregate composed of pyroxenes, olivine, and spinel (mainly clinopyroxene). These fine-grained zones seem to be recrystallized from bent pyroxene. Coarse-grained olivine is less deformed than pyroxenes, and only shows kink bands and weak wavy extinction. Coarse-grained spinel is very rare.

MINERAL CHEMISTRY

Minerals were analyzed using the JXA-5 type micro-analyzer of the Geological Institute, University of Tokyo. Correction methods are the same as those of Nakamura and Kushiro (1970). Except for spinel, iron was treated as ferrous. Ferric iron in spinel was calculated to bring RO/R_2O_3 to unity.

Olivine. The $Mg/(Mg + Fe^*)$ ratios of olivines range from 0.899 to 0.913 in Sample 18-1, 2C, and from 0.902 to 0.913 in Sample 18-2, 17B. As shown in Figure 1, olivines of Sample 18-1, 2C tend to be less magnesian than those of Sample 18-2, 17B. NiO contents are about 0.4 wt per cent in both samples. The composition of fine-grained granular olivine (the product of recrystallization) in Sample 18-2, 17B is nearly identical to that of the coarse-grained olivine (Table 1).

Orthopyroxene. The chemical compositions, carefully determined to avoid contamination of visible clinopyroxene lamellae, show that the $Mg/(Mg + Fe^*)$ ratio ranges from 0.899 to 0.912 (average 0.907), and the $Ca/(Ca + Mg + Fe^*)$ ratios are around 0.015 (Figure 2) in both samples. The averaged compositions of the central part of large orthopyroxene ("homogenized core" compositions), which may represent the compo-

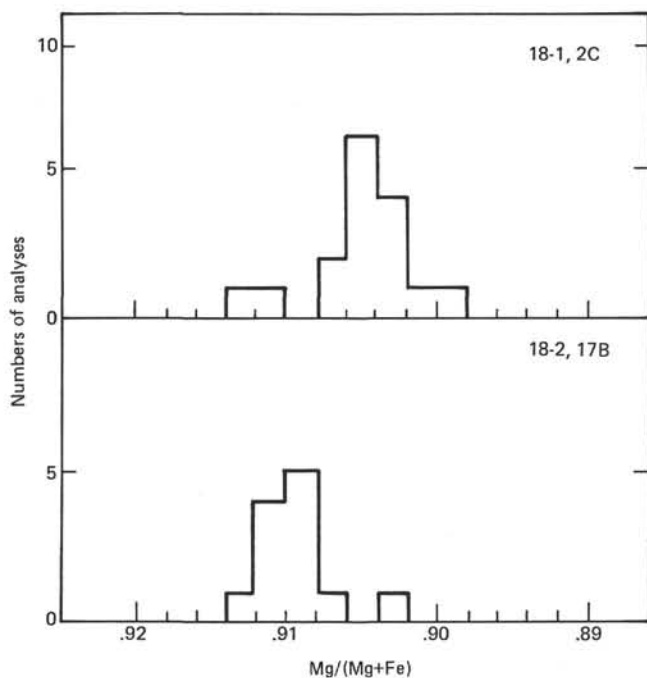


Figure 1. Histograms showing compositions of olivines.

TABLE 1
Selected Analyses of Olivines

	1	2	3	4	5	6	7	8
SiO ₂	39.8	39.7	40.4	40.6	40.3	40.1	39.8	39.5
Al ₂ O ₃	0.03	0.00	0.01	0.02	0.05	0.04	nd	nd
TiO ₂	nd	nd	0.00	0.00	0.00	0.00	nd	nd
FeO*	9.52	9.70	9.85	8.58	9.06	8.62	9.74	9.21
MnO	0.10	0.12	0.12	0.13	0.12	0.11	0.08	0.11
MgO	50.5	50.4	49.1	50.6	50.6	50.8	50.2	50.0
CaO	0.07	0.08	0.06	0.03	0.03	0.01	0.05	0.02
Na ₂ O	0.00	0.00	0.00	0.00	0.00	0.00	nd	nd
Cr ₂ O ₃	0.00	0.01	0.00	0.12	0.07	0.11	nd	nd
NiO	0.42	0.38	nd	nd	nd	nd	0.40	0.45
Total	100.4	100.4	99.5	100.1	100.2	99.8	100.3	99.3
Fo	90.4	90.2	89.9	91.3	90.9	91.3	90.2	90.6

Note: nd: not determined; (1) 01-2, 18-1; (2) 01-3, 18-1; (3) in contact with cpx, 18-1; (4) in contact with spinel, 18-1; (5) in contact with spinel, 18-2; (6) in contact with spinel, 18-2; (7) large olivine, 18-2; (8) fine-grained, granular, 18-2.

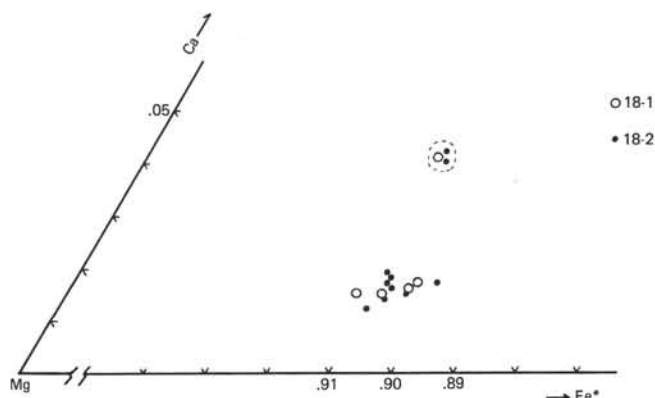


Figure 2. Compositions of orthopyroxenes plotted in the Mg-rich portion of the triangle Ca-Mg-Fe* (total iron as Fe). Those of "homogenized core" of the large grains are enclosed by a broken line.

sitions before exsolution, were estimated by averaging many broad-beam analyses (more than 20 points). Their $Ca/(Ca + Mg + Fe^*)$ ratios are around 0.04 (Figure 2), and the $Mg/(Mg + Fe^*)$ ratios range from 0.906 to 0.909 (average 0.908) in both samples.

The Al and Cr contents are higher in the "homogenized core" of large orthopyroxene and in orthopyroxene exsolution blebs in clinopyroxene than in the other orthopyroxene grain.

Clinopyroxene. The $Ca/(Ca + Mg + Fe^*)$ ratios of clinopyroxene in direct contact with orthopyroxene are all higher than 0.465. Some clinopyroxenes from Sample 18-2, 17B have slightly higher $Ca/(Ca + Mg + Fe^*)$ ratios than those from Sample 18-1, 2C (Figure 3). The $Mg/(Mg + Fe^*)$ ratios are higher than 0.92 in both samples. "Homogenized core" of clinopyroxene (host clinopyroxene + orthopyroxene lamellae) has noticeably low $Ca/(Ca + Mg + Fe^*)$ ratios (lower than 0.42). Its $Mg/(Mg + Fe^*)$ ratio is generally lower than 0.915 (average 0.913) in both Sample 18-1, 2C and Sample 18-2, 17B. The Na₂O content in clinopyroxene of Sample 18-1, 2C averages 0.2 wt per cent, and is about twice as high as that of Sample 18-2, 17B (Tables 2A and 2B).

The Al and Cr contents show a highly positive correlation with one another, and are especially high in

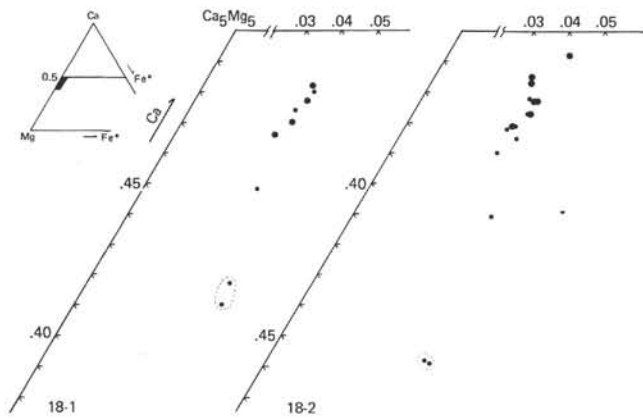


Figure 3. Compositions of clinopyroxenes plotted in the triangle Ca-Mg-Fe*. The large circles are the clinopyroxenes in direct contact with orthopyroxene. Compositions of "homogenized core" of the large grains are enclosed by broken lines.

the "homogenized core" of the large clinopyroxene (average 4.7 wt % Al₂O₃ and 1.5 wt % Cr₂O₃) and in clinopyroxene exsolution lamellae in orthopyroxene (Tables 2A and 2B).

Chromian spinel. Large spinel grains tend to be more chromian than the fine-grained ones intergrown with clinopyroxene in both samples. Chromian spinel in Sample 18-1, 2C is slightly more chromian than that in Sample 18-2, 17B; the Cr/(Cr+Al) ratio of the former is from 0.32 to 0.43, whereas that of the latter is

from 0.28 to 0.41 (Figure 4A). Mg/(Mg+Fe²⁺) ratio of chromian spinel ranges from 0.6 to 0.7 (Figure 4A; Table 3) in both samples. Ferric iron content is generally low, and the Fe³⁺/(Cr+Al+Fe³⁺) ratio never exceeds 0.05 (Figure 5A; Table 3). Chromian spinel rods in olivine, common in Sample 18-1, 2C, have compositions almost identical to the other types of spinel.

Chromian spinels of these samples are enriched in Al compared with those from harzburgite dredged at

TABLE 2A
Selected Analyses of Pyroxenes From 18-1 Lherzolite

	1	2	3	4	5	6	7	8
SiO ₂	51.1	50.0	54.2	53.6	51.4	54.9	51.1	55.2
Al ₂ O ₃	4.36	4.04	3.10	3.41	4.15	3.30	3.02	2.62
TiO ₂	0.13	0.12	0.03	0.07	0.16	0.05	0.10	nd
FeO*	3.33	2.47	6.16	6.17	2.58	6.44	2.75	6.38
MnO	0.09	0.04	0.11	0.12	0.08	0.10	0.04	nd
MgO	19.6	17.9	35.8	34.5	16.7	33.2	18.9	33.5
CaO	20.7	23.5	0.83	2.28	23.1	0.87	23.1	0.85
Na ₂ O	0.16	0.29	0.02	0.03	0.21	0.00	0.18	nd
Cr ₂ O ₃	1.48	1.41	0.89	0.95	1.40	0.86	0.85	0.66
Total	101.0	99.8	101.1	101.1	99.8	99.7	100.0	99.2
Numbers of atoms on O=6								
Si	1.844	1.838	1.862	1.853	1.879	1.908	1.869	1.925
Al ⁴	0.156	0.162	0.126	0.139	0.121	0.092	0.130	0.075
Al ⁶	0.030	0.013			0.058	0.037		0.033
Ti	0.004	0.003	0.001	0.002	0.004	0.001	0.003	
Fe*	0.101	0.076	0.177	0.178	0.079	0.187	0.084	0.186
Mn	0.003	0.001	0.003	0.003	0.003	0.003	0.001	
Mg	1.053	0.981	1.837	1.777	0.911	1.722	1.029	1.743
Ca	0.801	0.924	0.031	0.085	0.904	0.032	0.904	0.032
Na	0.011	0.020	0.001	0.002	0.015	0.000	0.013	
Cr	0.042	0.041	0.024	0.026	0.041	0.024	0.025	0.018
Mg	53.9	49.5	89.8	87.1	48.1	88.7	51.0	88.9
Ca	41.0	46.6	1.5	4.1	47.7	1.7	44.8	1.6
Fe	5.1	3.8	8.7	8.7	4.2	9.6	4.2	9.5

Note: nd: not determined; (1) 3-cpx "homogenized core"; (2) 3-cpx rim; (3) 3-opx rim; (4) 3-opx "homogenized core"; (5) cpx lamella of No. 6.; (6) opx host of No. 5.; (7) 2-cpx, fine-grained, intergrown with spinel; (8) 4-opx, in contact with chromian spinel.

TABLE 2B
Selected Analyses of Pyroxenes From 18-2 Lherzolite

	1	2	3	4	5	6	7	8	9	10
SiO ₂	51.1	54.5	53.7	50.1	55.5	52.5	55.8	52.2	54.7	51.7
Al ₂ O ₃	4.33	3.56	4.44	5.48	2.78	3.27	2.69	3.01	3.28	4.92
TiO ₂	0.12	0.00	0.03	0.13	0.05	0.16	0.01	0.06	0.07	0.14
FeO*	2.65	6.11	6.61	2.71	6.38	2.36	6.32	2.54	6.05	3.54
MnO	0.07	0.16	0.14	0.08	0.18	0.08	0.17	0.09	0.13	0.12
MgO	17.0	33.9	33.1	16.2	33.7	17.0	34.5	17.7	33.1	19.6
CaO	23.4	1.03	0.90	23.8	0.79	24.0	0.74	23.4	2.13	19.3
Na ₂ O	0.14	0.00	0.00	0.13	0.00	0.09	0.00	0.05	0.02	0.10
Cr ₂ O ₃	1.44	0.89	1.08	1.61	0.59	0.95	0.42	0.66	0.87	1.38
Total	100.3	100.2	100.0	100.0	100.0	100.4	100.7	99.7	100.4	100.8
Numbers of atoms on O=6										
Si	1.862	1.888	1.868	1.833	1.922	1.905	1.919	1.907	1.895	1.858
Al ⁴	0.138	0.113	0.132	0.167	0.078	0.095	0.081	0.093	0.105	0.142
Al ⁶	0.048	0.033	0.050	0.069	0.036	0.045	0.028	0.036	0.029	0.067
Ti	0.003	0.000	0.001	0.004	0.001	0.004	0.000	0.002	0.002	0.004
Fe*	0.081	0.177	0.192	0.083	0.185	0.072	0.182	0.078	0.175	0.107
Mn	0.002	0.005	0.004	0.003	0.005	0.002	0.005	0.003	0.004	0.004
Mg	0.924	1.751	1.715	0.881	1.739	0.921	1.767	0.962	1.711	1.049
Ca	0.916	0.038	0.034	0.933	0.030	0.934	0.027	0.917	0.079	0.743
Na	0.010	0.000	0.000	0.009	0.000	0.007	0.000	0.004	0.002	0.007
Cr	0.042	0.024	0.030	0.047	0.016	0.027	0.015	0.019	0.024	0.039
Mg	48.1	89.1	88.4	46.5	89.0	47.8	89.4	49.2	87.1	55.3
Ca	47.7	1.9	1.7	49.2	1.5	48.5	1.4	46.9	4.0	39.1
Fe	4.2	9.0	9.9	4.4	9.5	3.7	9.2	4.0	8.9	5.6

Note: (1) 7-cpx, lamella in No. 2; (2) 7-opx, host of No. 1; (3) 9-opx, bleb in No. 4, (4) 9-cpx, host of No. 3; (5) rim of a discrete grain, in contact with No. 6; (6) rim of a discrete grain, in contact with No. 5; (7) 5-opx, granular, in contact with No. 8; (8) 5-cpx, granular, in contact with No. 7; (9) "homogenized core" of a large grain; (10) "homogenized core" of a large grain.

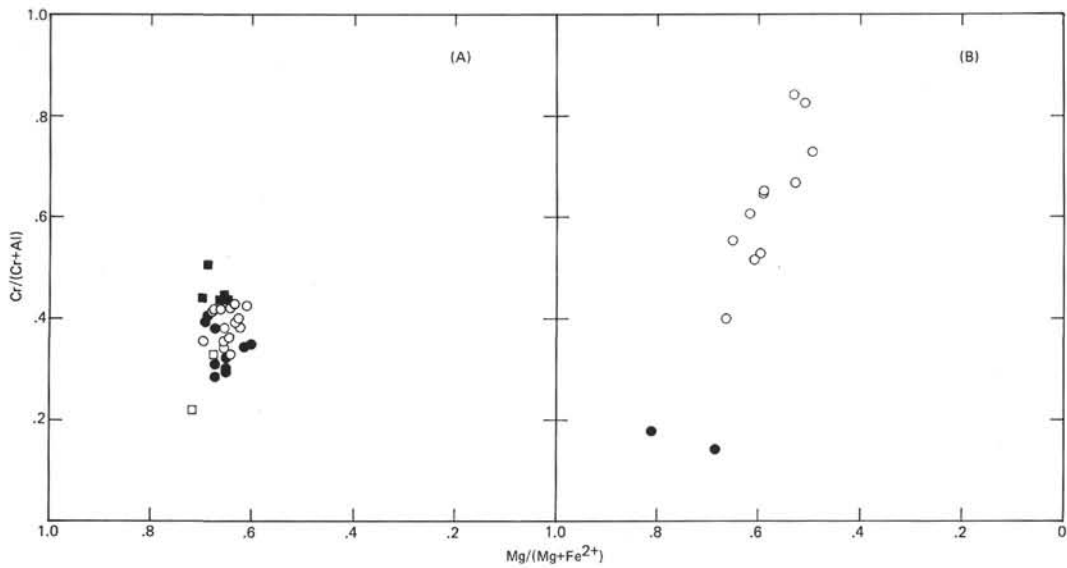


Figure 4. Compositions of spinels in the diagram $Cr/(Cr + Al) - Mg/(Mg + Fe^{2+})$. (A) Spinel from ultramafic rocks recovered near the Mid-Atlantic Ridge. Symbols: open circle, Sample 18-1, 2C; solid circle, Sample 18-2, 17B; open square, lherzolite from the Vema fracture zone (Prinz et al., 1976); solid square, harzburgite from 45°N on the Mid-Atlantic Ridge (Aumento and Loubat, 1971). (B) Spinel from the Newfoundland ophiolite complex. Symbols: open circle, harzburgite; solid circle, lherzolite.

45°N on the Mid-Atlantic Ridge (Aumento and Loubat, 1971), and are similar to or more chromian than those from lherzolite obtained from north of Vema fracture zone (Prinz et al., 1976) (Figures 4A and 5A).

When compared with spinels from the ultramafic tectonite of an ophiolite complex (Malpas and Strong, 1975) and those from lherzolite xenoliths in alkaline basalts and worldwide alpine peridotites, chromian spi-

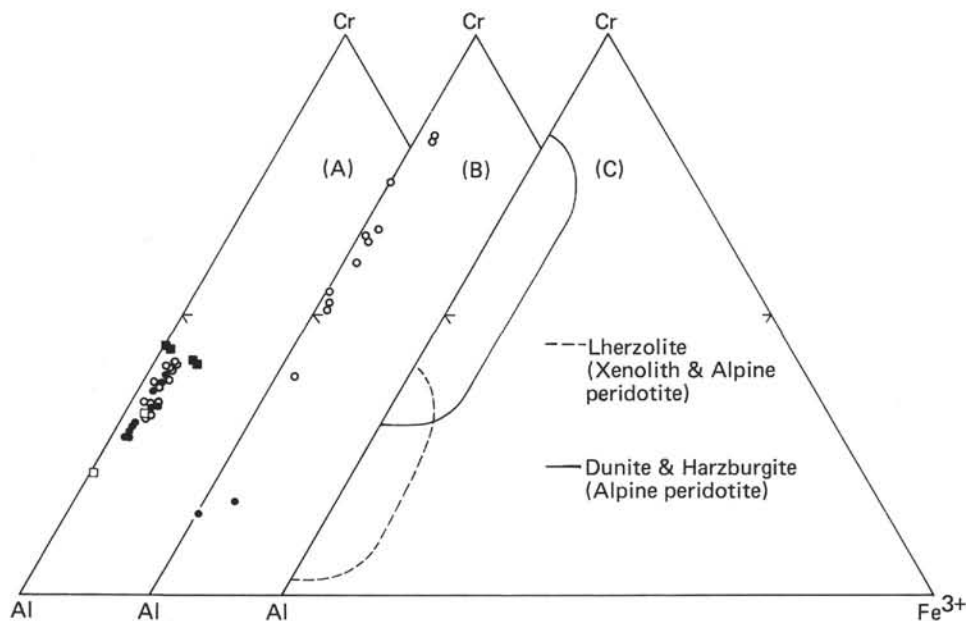


Figure 5. Compositions of spinels in the triangle $Cr-Al-Fe^{3+}$. (A) Spinel from ultramafic rocks recovered near the Mid-Atlantic Ridge. Symbols are the same as for Figure 4A. (B) Spinel from the Newfoundland ophiolite complex. Symbols are the same as for Figure 4B. (C) Compositional fields of spinels from Alpine-type dunite-harzburgite and from lherzolites of Alpine-type and of xenoliths in basaltic rocks. References are in Appendix.

nels from oceanic peridotites show the transitional compositions between those of hercynite and harzburgite in the Cr/(Cr+Al) and Mg/(Mg+Fe²⁺) ratios (Figures 4B, 5B, and 5C).

TABLE 3
Selected Analyses of Chromian Spinel

	1	2	3	4	5
SiO ₂	0.05	0.04	0.10	0.00	0.14
Al ₂ O ₃	32.6	33.2	31.7	38.0	36.1
TiO ₂	0.07	0.14	0.12	0.05	0.04
FeO*	17.2	15.8	17.9	18.5	18.2
MnO	0.35	0.28	0.31	0.33	0.31
MgO	14.6	15.5	14.2	15.3	14.8
CaO	0.19	0.01	0.01	0.01	0.01
Na ₂ O	nd	0.00	0.02	nd	0.04
Cr ₂ O ₃	34.8	35.7	35.4	28.4	30.6
NiO	0.11	0.15	0.08	0.15	nd
Total	100.0	100.8	99.8	100.7	100.2
Numbers of atoms on 0=4					
Si	0.002	0.001	0.003	0.000	0.004
Al	1.131	1.138	1.113	1.282	1.232
Ti	0.002	0.003	0.003	0.001	0.001
Fe*	0.423	0.385	0.445	0.444	0.441
Mn	0.009	0.007	0.008	0.008	0.008
Mg	0.641	0.672	0.631	0.653	0.641
Ca	0.006	0.000	0.000	0.000	0.000
Cr	0.811	0.822	0.833	0.645	0.700
Ni	0.003	0.003	0.002	0.004	
Mg/Mg+Fe''	0.640	0.668	0.627	0.648	0.638
Cr	0.405	0.409	0.413	0.320	0.348
Al	0.564	0.566	0.552	0.636	0.613
Fe'''	0.031	0.025	0.034	0.044	0.039

	6	7	8	9	10
SiO ₂	0.02	0.04	0.09	0.16	0.12
Al ₂ O ₃	33.7	35.7	39.6	42.1	40.9
TiO ₂	0.13	0.08	0.05	0.04	0.01
FeO*	15.7	16.1	16.8	15.9	15.8
MnO	0.35	0.33	0.32	0.24	0.27
MgO	15.9	15.6	15.3	15.9	16.1
CaO	0.00	0.00	0.01	0.02	0.09
Na ₂ O	0.00	0.00	0.04	0.00	0.02
Cr ₂ O ₃	34.7	32.0	27.7	25.0	27.4
NiO	nd	nd	nd	nd	nd
Total	100.5	99.9	99.9	99.4	100.7

	6	7	8	9	10
Numbers of atoms on 0=4					
Si	0.001	0.001	0.003	0.005	0.003
Al	1.151	1.218	1.331	1.401	1.351
Ti	0.003	0.002	0.001	0.001	0.000
Fe*	0.380	0.391	0.401	0.376	0.371
Mn	0.009	0.008	0.008	0.006	0.006
Mg	0.685	0.671	0.649	0.671	0.675
Ca	0.000	0.000	0.000	0.001	0.003
Cr	0.796	0.731	0.625	0.557	0.607
Mg/Mg+Fe''	0.683	0.669	0.648	0.670	0.674
Cr	0.396	0.365	0.312	0.278	0.303
Al	0.573	0.609	0.664	0.700	0.675
Fe'''	0.030	0.026	0.024	0.022	0.022

Note: nd: not determined; (1) fine-grained spinel intergrown with cpx, 18-1; (2) core of a large anhedral grain, 18-1; (3) protruded "arm" of No. 2, 18-1; (4) 2-spinel, in contact with secondary magnetite, 18-1; (5) fine-grained spinel intergrown with cpx, 18-1; (6) core of a large anhedral grain, 18-2; (7) protruded "arm" of No. 6, 18-2; (8) 11-spinel, in contact with opx, 18-2; (9) 12-spinel, in contact with olivine, 18-2; (10) 1-spinel, granular, fine-grained, and associated with clinopyroxene, 18-2.

ESTIMATION OF TEMPERATURES

The partition of Mg and Fe between clinopyroxene and orthopyroxene is sensitive to equilibration temperature, and the partition coefficient, $K_D^{cpx-opx} = (X_{Mg}^{cpx} / X_{Fe}^{cpx}) \cdot (X_{Fe}^{opx} / X_{Mg}^{opx})$, decreases with increasing equilibration temperature (e.g., Kretz, 1961). Two kinds of clinopyroxene-orthopyroxene pairs are obtained from Sample 18-1, 2C and 18-2, 17B peridotites: one is the pair of two discrete pyroxenes in contact with one another, and the other is the pair of clinopyroxene lamella (bleb) and orthopyroxene host, or vice versa. Obtained K_D values (Table 4) are around 1.2 or 1.3 in both Samples 18-1, 2C and 18-2, 17B, although K_D values of the lamella-host pairs in Sample 18-2, 17B (average 1.16) seem a little smaller than those of other pairs. In Sample 18-2, 17B, K_D values of discrete pairs both from the fine-grained granular part and from the coarse-grained part give the nearly same value. It is noteworthy that the K_D values of the core-core pairs of large discrete pyroxene ("homogenized core") are considerably lower (1.05 in Sample 18-1, 2C and 1.07 in Sample 18-2, 17B), indicating the high temperature of equilibration (e.g., Kretz, 1961).

The K_D values for experimental magnesian pyroxene pairs are around 1.1 at about 1100°C (Akella and Boyd, 1973; Hensen 1973) and about 0.9 at 1410°C (Hensen, 1973), assuming no ferric iron in pyroxenes. On the basis of the above experimental results, the K_D value of 1.2 or 1.3 probably denotes temperatures around 900°C. On the other hand, the K_D value

TABLE 4
Determined K_D 's of Partitioning of Mg-Fe (total iron) Between Clinopyroxene and Orthopyroxene, and Between Clinopyroxene and Olivine

Sample	$K_D^{cpx-opx}$ (Mg-Fe)	Occurrence of the Pair
18-1	1.22	discrete-discrete
	1.25	discrete-discrete
	(1.05)	"homogenized core"
18-2	1.25	discrete-discrete
	1.27	cpx lamella in opx
	1.12	cpx lamella in opx
	1.33	discrete-discrete
	1.37	discrete-discrete
	(1.07)	"homogenized core"
	1.27	discrete-discrete
		fine-grained, granular
	1.31	discrete-discrete
		fine-grained, granular
	1.15	cpx lamella in opx
	1.16	cpx lamella in opx
	1.16	cpx lamella in opx
	1.16	cpx transudation around opx
	1.19	opx bleb in cpx
Sample K_D^{cpx-ol} (Mg-Fe)		
18-1	1.18, 1.24, 1.25, 1.29 and 1.32	
18-2	1.19, 1.21, 1.22, 1.27 and 1.28	

smaller than 1.1 of "homogenized core" pairs indicates temperature in excess of 1100°C, and may indicate the temperature of igneous activity prior to recrystallization.

Partition of Fe and Mg between olivine and clinopyroxene is also sensitive to temperature. The partition coefficient, $K_D^{cpx-ol} = (X_{Mg}^{cpx}/X_{Fe}^{cpx}) \cdot (X_{Fe}^{ol}/X_{Mg}^{ol})$, increases with decreasing temperature (e.g., O'Hara and Mercy, 1963); a simple relation between the K_D value and temperature cannot be obtained, however, probably because of the composition dependence of the K_D value (Obata et al., 1974; Wood, 1976). When the Mg/(Mg+Fe*) ratios of olivine and clinopyroxene pairs are plotted in a Roseboom diagram, (Figure 6) however, it is possible to deduce approximate equilibration temperature by comparison with other pairs of known temperatures (Mori and Banno, 1973). The olivine-clinopyroxene pairs from both Samples 18-1, 2C and 18-2, 17B peridotites fall in the region between those from Seiad and Finero ultramafic complexes (Medaris, 1975) and the line which represents a partition coefficient of unity, indicating they may have been equilibrated at temperatures higher than 750°C (Medaris, 1975). The olivine-clinopyroxene pairs from lherzolite inclusions in an alkaline basalt (Frey and Green, 1974) fall in almost the same region as those studied here. Frey and Green (1974) argued that the lherzolite inclusions were equilibrated at temperatures lower than 1050°C. From the above discussion, we suggest that olivine-clinopyroxene pairs from the peridotites of Samples 18-1, 2C and 18-2, 17B were equilibrated at temperatures between 750°C and 1050°C, and probably at 900°C.

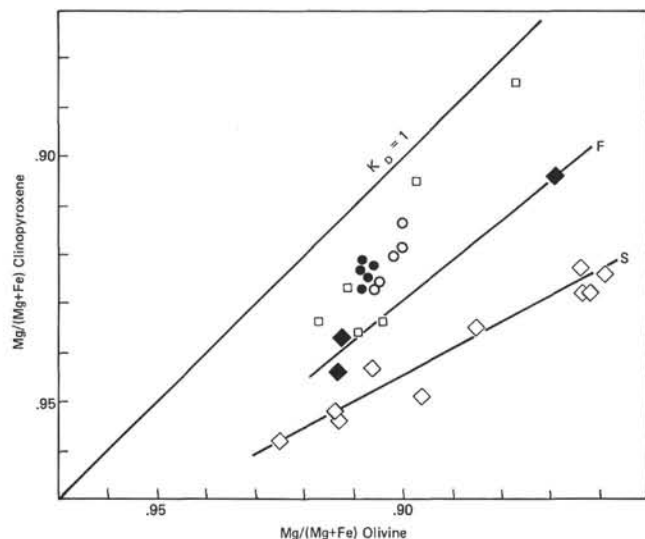


Figure 6. Mg-Fe partitioning between clinopyroxene and olivine. Symbols: open circle, Sample 18-1, 2C; solid circle, Sample 18-2, 17B; open square, lherzolite xenoliths in an alkaline basalt (Frey and Green, 1974); solid diamond, Finero complex (Medaris, 1975); open diamond, Seiad complex (Medaris, 1975).

Although an olivine-spinel geothermometer was developed by Irvine (1965) and Jackson (1969), temperatures estimated by their methods seem too high and no experimental calibration is available. For comparative purposes, however, Fe-Mg partition between olivine and spinel should be useful. As shown in Figure 7, the olivine-spinel pairs from both Samples 18-1, 2C and 18-2, 17B peridotites fall in the region between those from Seiad and Finero ultramafic complexes and those from lherzolite inclusions in the west Victoria alkaline basalt (Frey and Green, 1974), which suggests that the equilibration temperature of these oceanic peridotites is between 750°C and 1050°C (Medaris, 1975; Frey and Green, 1974).

DISCUSSION

It is not clear whether these peridotites were emplaced into their present position in the oceanic crust by intrusion along a fault or were derived as sedimentary fragments from a peridotite body first exposed at the surface along a fault scarp, then covered by later lava flows. It is important, however, that serpentinized peridotites were recovered at the shallower portion of oceanic crust at Site 395, where no major fracture zone exists nearby. This may support the theory that serpentinized peridotite is a significant component of the normal oceanic crust, where it is emplaced by vertical intrusion into a fault zone (Bonatti and Honnorez, 1976).

The internal consistency of the estimated equilibration temperatures implies that peridotites in Samples 18-1, 2C and 18-2, 17B were well equilibrated at subsolidus temperature (less than 1000°C, probably 900°C). Such temperatures are too high for oceanic crust, and it is most likely that these peridotites were equilibrated in the oceanic upper mantle, then intruded into the oceanic crust along faults as solid intrusions.

There is no evidence that these two samples are cumulates from mafic or ultramafic magma. Considering

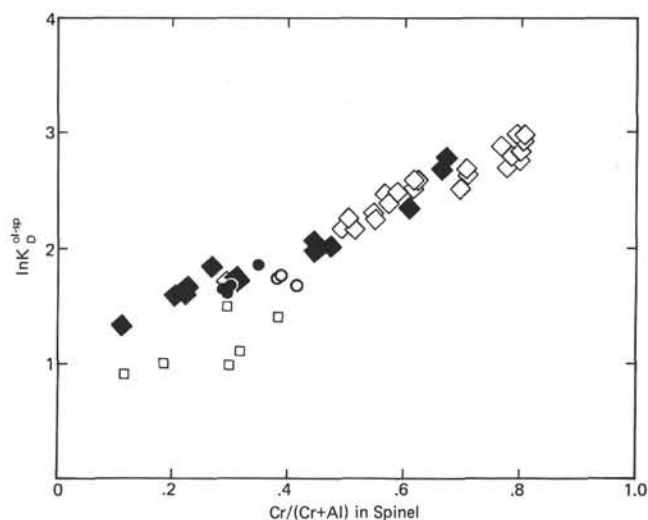


Figure 7. Mg-Fe partitioning between spinel and olivine. Symbols are the same as for Figure 6.

that olivine and pyroxene are very magnesian [(Mg/(Mg+Fe*)) ratios are higher than 0.9], that K-bearing minerals are absent, and that Na content in clinopyroxene and consequently in bulk compositions is very low. Samples 18-1, 2C and 18-2, 17B may be residual oceanic upper mantle left after removal of more easily fusible components as basaltic magmas.

Among the ultramafic rocks recovered near the Mid-Atlantic Ridge, an entire spectrum exists, from the lherzolite to the harzburgite subtypes (e.g., Aumento and Loubat, 1971; Prinz et al., 1976), and most, including two samples studied here, show the prominent deformation and recrystallization textures and a residual bulk compositional character commonly recognized in ultramafic tectonites of ophiolite complexes. Furthermore, ultramafic rocks corresponding to the ultramafic cumulates of the ophiolite complex have been also obtained at DSDP Site 334 (Hodges and Papike, 1976). It is probable, therefore, that the ophiolite complexes for the future are produced at or near the Mid-Atlantic Ridge, and the peridotites studied here are of such an ophiolite complex of the future.

Although the similarity between the tectonites of the ophiolite complexes and the ultramafic rocks from the Mid-Atlantic Ridge was emphasized above, there are some differences. In the tectonites of the ophiolite complexes, dunite and harzburgite subtypes are predominant and lherzolite and lherzolititic harzburgite are rare (e.g., Malpas and Strong, 1975), whereas lherzolite or lherzolititic harzburgite seem to be more common in the Mid-Atlantic Ridge region (e.g., Prinz et al., 1976). In this sense, the stratigraphic section of the Mid-Atlantic Ridge region may be different from that of the ophiolite complex. The difference may be only apparent, however, because all the ultramafic rocks of the Mid-Atlantic Ridge region were recovered from the shallow portion of the oceanic crust or from fracture zones, and consequently they do not always represent the spectrum of the normal oceanic upper mantle.

Another difference is the equilibration temperature. Most peridotites from ultramafic tectonites of ophiolite complexes are equilibrated near 700°C (e.g., Medaris, 1975), whereas the samples studied here show higher equilibration temperatures. The low equilibration temperatures of ultramafic tectonites are believed by some (e.g., Medaris, 1975) to result from the effect of regional metamorphism which took place after they migrated with oceanic crust at the converging plate boundaries. Considering that ultramafic tectonites indicate higher equilibration temperature (e.g., granulite facies) than the surrounding basic rocks (e.g., green schist or amphibolite facies), however, such interpretation may not be correct. It is more likely that ultramafic complexes generated near the mid-oceanic ridges cool to about 700°C during transport from the mid-oceanic ridges to converging boundaries, because the thermal gradient of oceanic upper mantle becomes more gentle toward the marginal part (e.g., Solomon, 1976). The peridotite complexes then are emplaced as cold tectonites at the converging plate boundaries to form ophiolite complexes. If regional metamorphism

continues after emplacement, those ultramafic tectonites may be equilibrated at a temperature similar to the surrounding basic rocks, as is the case of Mt. Higashi-Akaishi (Mori and Banno, 1973). If the metamorphism does not continue, those ultramafic tectonites show an equilibration temperature higher than the surrounding basic rocks, as is the case of Finero complex (Medaris, 1975).

ACKNOWLEDGMENTS

The authors are indebted to Drs. B. O. Mysen and N. T. Arndt for their critical review and useful suggestions.

REFERENCES

- Akella, J. and Boyd, F. R., 1973. Effect of pressure on the composition of coexisting pyroxenes and garnet in the system $\text{CaSiO}_3\text{-MgSiO}_3\text{-FeSiO}_3\text{-CaAlTi}_2\text{O}_6$, *Carnegie Inst. Wash. Yearbook*, v. 72, p. 523-526.
- Aumento, F. and Loubat, H., 1971. The mid-Atlantic Ridge near 45°N. XVI. Serpentinized ultramafic intrusions, *Canadian J. Earth Sci.*, v. 8, p. 631-663.
- Basu, A. R., 1977. Olivine-Spinel equilibria in lherzolite xenoliths from San Quintin, Baja California, *Earth Planet Sci. Lett.*, v. 33, p. 443-450.
- Bonnatti, E. and Honnorez, J., 1976. Sections of the earth's crust in the equatorial Atlantic, *J. Geophys. Res.*, v. 81, p. 4105-4116.
- Coleman, R. G., 1971. Plate tectonic emplacement of upper mantle peridotites along continental edges, *J. Geophys. Res.*, v. 76, p. 1212-1222.
- Frey, F. A. and Green, D. H., 1974. The mineralogy, geochemistry and origin of lherzolite inclusions in Victorian basanites, *Geochim. Cosmochim. Acta*, v. 38, p. 1023-1059.
- Hensen, B. J., 1973. Pyroxenes and garnets as geothermometers and barometers, *Carnegie Inst. Wash. Yearbook*, v. 72, p. 527-534.
- Hodges, F. N. and Papike, J. J., 1976. DSDP Site 334: Magmatic cumulates from oceanic Layer 3, *J. Geophys. Res.*, v. 81, p. 4135-4151.
- Irvine, T. N., 1965. Chromian spinel as a petrogenetic indicator. Part 1—Theory, *Canadian J. Earth Sci.*, v. 2, p. 648-674.
- Jackson, E. D., 1969. Chemical variation in coexisting chromite and olivine in chromitite zones of the Stillwater Complex, *Econ. Geol. Monogr.*, v. 4, p. 41-71.
- Kretz, R., 1961. Some applications of thermodynamics to coexisting minerals of variable composition. Examples: orthopyroxene-clinopyroxene and orthopyroxene-garnet, *J. Geol.*, v. 69, p. 361-387.
- Malpas, J. and Strong, D. F., 1975. A comparison of chromespinels in ophiolites and mantle diapirs of Newfoundland, *Geochim. Cosmochim. Acta*, v. 39, p. 1045-1060.
- Medaris, L. G., 1975. Coexisting spinel and silicates in alpine peridotites of the granulite facies, *Geochim. Cosmochim. Acta*, v. 39, p. 947-958.
- Miyashiro, A., 1973. The Troodos ophiolitic complex was probably formed in an island arc, *Earth Planet. Sci. Lett.*, v. 19, p. 218-224.
- Moores, E. M. and Vine, F. J., 1971. The Troodos massif, Cyprus and other ophiolites as oceanic crust: evaluation and implications, *Phil. Trans. Royal Soc. London*, ser. A, v. 268, p. 443-466.
- Mori, T. and Banno, S., 1973. Petrology of peridotite and garnet clinopyroxenite of the Mt. Higashi-Akaishi mass, central Shikoku, Japan—subsolidus relation of anhydrous phases, *Contrib. Mineral. Petrol.*, v. 41, p. 301-323.

- Nakamura, Y. and Kushiro, I., 1970. Compositional relations of coexisting orthopyroxene, pigeonite and augite in a tholeiitic andesite from Hakone volcano, *Contrib. Mineral. Petrol.*, v. 26, p. 265-275.
- Obata, M., Banno, S., and Mori, T., 1974. The iron-magnesium partitioning between naturally occurring coexisting olivine and Ca-rich clinopyroxene: an application of the simple mixture model to olivine and solution, *Bull. Soc. franc. Minéral. Crist.*, v. 97, p. 101-107.
- O'Hara, M. J. and Mercy, E. L. P., 1963. Petrology and petrogenesis of some garnetiferous peridotites, *Trans. Roy. Soc. Edinburgh*, v. 65, p. 251-314.
- Prinz, M., Keil, K., Green, J. A., Reid, A. M., Bonatti, E., and Honnorez, J., 1976. Ultramafic dredged samples from the equatorial Mid-Atlantic Ridge and fracture zones, *J. Geophys. Res.*, v. 81, p. 4087-4103.
- Solomon, S. C., 1976. Geophysical constraints on radial and lateral temperature variations in upper mantle, *Am. Mineralogist*, v. 61, p. 788-803.
- Wood, B. J., 1976. An olivine-clinopyroxene geothermometer: A discussion, *Contrib. Mineral. Petrol.*, v. 56, p. 297-303.
- Green, D. H., 1964. The petrogenesis of the high-temperature peridotite intrusion in the Lizard area, Cornwall, *J. Petrol.*, v. 5, p. 134-188.
- Hamad, S. el D., 1963. The chemistry and mineralogy of the olivine nodules of Calton Hill, Derbyshire, *Min. Mag.*, v. 33, p. 483-497.
- Himmelberg, G. R. and Coleman, R. G., 1968. Chemistry of primary minerals and rocks from the Red Hill-Del Puerto ultramafic mass, California, *U.S.G.S. Prof. Paper*, 600-C, p. 18-26.
- Himmelberg, G. R. and Loney, R. A., 1973. Petrology of the Vulkan Peak Alpine-type peridotite, southwestern Oregon, *Geol. Soc. Am. Bull.*, v. 84, p. 1585-1600.
- Irving, A. J., 1974. Pyroxene-rich ultramafic xenoliths in the newer basalts of Victoria, Australia, *N. Jb. Min.*, v. 120, p. 147-167.
- Komatsu, M., 1975. Recrystallization of the high-alumina pyroxene peridotite of the Uenzaru area in Hidaka province, Hokkaido, Japan, *J. Geol. Soc. Japan*, v. 81, p. 11-28.
- Kornprobst, J., 1966. A propos des péridotites du Massif des Beni-Bouchera (Rif septentrional, Maroc), *Bull. Soc. franc. Minéral. Crist.*, v. 89, p. 399-404.
- Littlejohn, A. L. and Greenwood, H. J., 1974. Lherzolite nodules in basalts from British Columbia, Canada, *Canadian J. Earth Sci.*, v. 11, p. 1288-1308.
- Loney, R. A., Himmelberg, G. R., and Coleman, R. G., 1971. Structure and petrology of the Alpine-type peridotite at Burro Mountain, California, U.S.A., *J. Petrol.*, v. 12, p. 245-309.
- MacGregor, I. D. and Smith, C. H., 1963. The use of chrome spinels in petrographic studies of ultramafic intrusions, *Canadian Min.*, v. 7, p. 403-412.
- Medaris, L. G., 1972. High-pressure peridotites in southwestern Oregon, *Geol. Soc. Am. Bull.*, v. 83, p. 41-58.
- Miller, R. III, 1953. The Webster-Addie ultramafic ring, Jackson County, North Carolina, and secondary alteration of its chromite, *Am. Mineralogist*, v. 38, p. 1134-1147.
- Monchoux, P. and Besson, M., 1969. Sur les compositions chimiques des minéraux des lherzolites pyrénéennes et leur significances génétique, *Bull. Soc. franc. Min. Crist.*, v. 92, p. 289-298.
- O'Hara, M. J., Richardson, S. W., and Wilson, G., 1971. Garnet-peridotite stability and occurrence in crust and mantle, *Contrib. Mineral. Petrol.*, v. 32, p. 48-68.
- Rio, M., 1968. Quelques précisions sur la composition minéralogique de la lherzolite de Moun Caou (Basses-Pyrenées), *Bull. Soc. franc. Minéral. Crist.*, v. 91, p. 298-299.
- Ross, C. S., Foster, M. D., and Myers, A. T., 1954. Origin of dunites and of olivine-rich inclusions in basaltic rocks, *Am. Mineralogist*, v. 39, p. 693-737.

APPENDIX

References Not Cited in the Text but Used to Construct Figure 5C

- Aoki, K. and Prinz, M., 1974. Chromian spinels in lherzolite inclusions from Itinome-gata, Japan, *Contrib. Mineral. Petrol.*, v. 46, p. 249-256.
- Arai, S., 1976. Petrology of Alpine-type ultramafic complexes in Sangun zone, western Japan. Unpublished thesis, University of Tokyo.
- Basu, A. R., 1975. Hot-spots, mantle plumes and a model for the origin of ultramafic xenoliths in alkali basalts, *E.P.S.L.*, v. 28, p. 261-274.
- Basu, A. R. and MacGregor, I. D., 1975. Chromite spinels from ultramafic xenoliths, *Geochim. Cosmochim. Acta*, v. 39, p. 937-945.
- Best, M. G., 1974. Contrasting types of chromium-spinel peridotite xenoliths in basaltic lavas, western Grand Canyon, Arizona, *E.P.S.L.*, v. 23, p. 229-237.
- Challis, G. A., 1965. The origin of New Zealand ultramafic intrusions, *J. Petrol.*, v. 14, p. 113-131.